05

Plasmon-polaritons at the interface of superconducting and non-superconducting artificial diamond

© V.A. Kukushkin,[1,2] Yu.V. Kukushkin[2]

[1] Federal Research Center A.V. Gaponov-Grekhov Institute of Applied Physics of the Russian Academy of Sciences, 603950 Nizhny Novgorod, Russia
[2] Lobachevsky University of Nizhny Novgorod, 603022 Nizhny Novgorod, Russia
e-mail:vakuk@ipfran.ru

Received June 24, 2025
Revised September 6, 2025
Accepted September 12, 2025

The theoretical estimates of the characteristics of surface plasmon-polaritons at the interface of highly boron-doped superconducting and non-superconducting diamond are obtained. It is shown that at temperatures significantly lower than the critical temperature of the superconducting transition and frequencies below the threshold for breaking Cooper pairs of holes (approximately 300 GHz) they have negligibly small Ohmic dissipation. At the threshold frequency, their wavelength and the scale of transverse localization of their electromagnetic field is of the order of 1 nm, which is more than a million times smaller than the vacuum wavelength corresponding to this frequency. At these frequencies, the existence of Ohmically non-dissipative localized states of surface plasmon-polaritons on non-superconducting doped diamond nanoparticles embedded in superconducting doped diamond is also possible. At a temperature near the critical value (specifically 10% lower than it), the threshold frequency of surface plasmon-polaritons decreases to approximately 150 GHz. In addition they become Ohmically dissipative with a field absorption length of the order of and more than 7 μm, which exceeds their wavelength only at frequencies below approximately 100 GHz. Minimal wavelength and the scale of their transverse localization are also achieved at the threshold frequency and equal 11 and 6 μm microns correspondingly. The localized states of plasmon-polaritons on non-superconducting doped diamond nanoparticles embedded in superconducting doped diamond also become Ohmically dissipative and have a quality factor greater than unity only in a narrow range (near $3.76 \cdot 10^{20}\,\mathrm{cm}^{-3}$) of boron dopant concentrations in these particles.

Keywords: boron doping, Cooper pair, diamond, insulator-metal transition, plasmon-polariton, superconductivity.

DOI: 10.61011/TP.2026.02.62879.160-25

Introduction

Surface plasmon polaritons are self-coherent electromagnetic field and polarization oscillations localized at an interface between two media (usually metal-dielectric) with unlike signs of real parts of their permittivities [1]. Near the so-called plasmon polariton resonance (when these parts are equal to each other in the absolute value), scales of such localization in direction orthogonal to this boundary and a wavelength in direction parallel to this interface can be much smaller than a radiation wavelength with a corresponding frequency in each of these media separately. Thus, small sizes of micro- and nanoelectronic circuits can be adapted to relatively long distances, at which the electromagnetic field of optical and infrared frequency ranges in homogeneous media. As a result it is possible to effectively use radiation of this frequency region characterized by a large amount of sources in nanooptical devices.

Electric field and polarization oscillations can be also localized on metal particles in a dielectric or on dielectric particles in a metal, sizes of which (and consequently, the localization scale in all three space coordinates) are much smaller than the wavelengths corresponding to their frequencies in each of these media separately [1] (localized states of surface plasmon polaritons). This drives important applications of plasmons such as field-based Raman enhancement of electromagnetic radiation on molecules, molecular fluorescence, nonlinear multiple harmonic generation, electromagnetic radiation transmission through subwavelength holes (and creation of sensors based on the sensitivity of this transmission gain to external impacts), development of spectroscopic chemical sensors (including biological media sensors) with nanometer resolution, which use the dependence of plasmon polariton resonance in such particles on permittivity of their immediate neighborhood, etc.

However, all these applications have a problem of matching high space localization of surface plasmon polaritons and long length of their ohmically dissipativeless propagation: the higher the degree of this localization the larger their attenuation coefficient. This is due to the fact that the higher localization the more part of surface plasmon polariton energy is contained in metal and, consequently, is prone to dissipation owing to finite conductivity of the latter. Compensation of this dissipation due to the amplification medium (or even self-generation of surface

plasmon polaritons, i.e. creation of plasmon polariton laser, so-called spaser) makes the corresponding devices much more sophisticated [2–4].

Therefore it is interesting to use superconducting, rather than normal, metal as a negative permittivity medium. This is due to the fact that for superconductors at sufficiently low frequencies (when the photon energy is insufficient for breaking Cooper pairs) at temperatures much lower than the critical superconducting transition temperature, the imaginary part of permittivity is small and disappears as the temperature approaches absolute zero [5–7]. Consequently, surface plasmon polaritons at the superconducting metal — dielectric interface will have a longer ohmically dissipativeless propagation length, and localized states of surface plasmon polaritons on superconducting metal or dielectric nanoparticles have narrow resonance lines. These properties of plasmon polaritons in superconducting structures have been of much interest to researchers [9–15] since their first experimental demonstration in 1994 [8].

However, due to mismatching between metal and dielectric lattice parameters, metal-dielectric interface will have nonuniformities, which will scatter plasmon polaritons and degrade the performance of plasmon-polariton-based devices. Therefore, a contact between heavily doped and weakly doped semiconductors with the same main chemical composition is very interesting. Due to coherence of their lattices, such contact can be considered to be defectless. At the same time heavily doped semiconductors, in which insulator–metal phase transition has occurred to a state with metallic (i.e. temperature-independent) conductivity [16] with sufficiently low temperatures, can become superconductors [17–23].

One of the most promising semiconductors for this purpose is the artificial diamond having unique properties (high thermal conductivity and mechanical strength, radiation and chemical resistance, etc.). Superconductivity in heavily boron-doped (to concentration of the order of $10^{21}\,\mathrm{cm}^{-3}$ and higher, where the insulator–metal phase transition has already taken place) artificial diamond at temperatures of the order of liquid helium and lower, was discovered in 2004 [24]. Possible modulation of the degree of doping with a rate of about 1 decade/nm [25,26] and the absence of proximity effect[1] [27] demonstrate that a sharp superconducting–non-superconducting doped diamond interface is essentially achievable which is necessary for creating plasmon polariton devices with record-breaking performance.

This work is devoted to theoretical investigation of the properties of surface plasmon polaritons and their localized states at the interface between more boron-doped (and therefore superconducting) and less boron-doped (and therefore dielectric) artificial diamond. For this, Section 1 describes a model of permittivity of superconducting and non-superconducting doped diamond in the temperature range from critical to zero temperature. Section 2 shows the main equations describing the surface plasmon polariton dispersion law and eigen frequencies of localized states of plasmon polaritons. In Section 3, equations from Sections 1 and 2 were used to evaluate the properties of surface plasmon polaritons and their localized states at the interface between the superconducting and non-superconducting doped diamond. In the Conclusion, the findings being of interest for promising applications are summarized.

1. Permittivity of superconducting and non-superconducting doped diamond

Consider a case without non-superconducting holes, i.e. the temperature T is much lower than the critical superconducting transition temperature T_{cr}, which is, for heavily boron-doped diamond, near the liquid helium temperature of 4.2 K [28]. We consider the case $l \ll \xi_0 = \hbar v/\Delta_0$, which is common for the superconducting doped diamond, where $l = \tau v$ is the hole free path with respect to elastic scattering by dopant atoms, τ is the corresponding transport time, v is the Fermi velocity of holes, ξ_0 is the coherence length (Cooper pair size) of holes at zero temperature and without impurities, $\hbar$ is the Planck constant, Δ_0 is the band gap in the elementary excitation spectrum of superconducting holes at zero temperature according to the Bardeen–Cooper–Schrieffer theory [29] (adequately describing the superconducting boron-doped diamond [28]) approximately equal to $2k_{\mathrm{B}}T_{\mathrm{cr}}$, k_{B} is the Boltzmann constant.

Suppose also that $kl \leq 1$, where k is the electromagnetic wavenumber, which makes it possible to neglect space dispersion. Then, according to [5], relative permittivity of superconducting holes at low electromagnetic field frequencies $\omega < 2\Delta_0/\hbar$, where the photon energy is insufficient for breaking the hole Cooper pair, is given by the following equation

$$\varepsilon_1 \approx \varepsilon - \frac{\pi\sigma\Delta_0}{\varepsilon_0\hbar\omega^2}. \qquad (1)$$

Here, $\varepsilon \approx 5.4$ is the relative static permittivity of diamond lattice [30], ε_0 is the electric constant, $\sigma = e^2N\tau/m$ is the static (because from $l \ll \xi_0$ and $\omega < 2\Delta_0/\hbar$ it follows that $\omega\tau \ll 1$) conductivity of holes at above-critical temperature resulting from elastic scattering by dopant atoms, e — is the hole charge equal to the elementary charge, N is the hole concentration, m is the effective hole mass equal by the order of magnitude to the free electron half-mass [30]. Other numeric values of parameters included in (1) are given in Section 3.

At temperatures of the order of the critical temperature, in the numerator of equation for ε_1 it is necessry to replace the full concentration of holes N (which is included there via σ) with the concentration of superconducting holes $N_s < N$ and add a term describing the contribution of non-superconducting holes with the concentration $N_n \equiv N - N_s$ [27]. As a result, when $\omega < 2\Delta/\hbar$ (where the band gap Δ in the elementary excitation spectrum

[1] The proximity effect is absent because the insulator–metal transition hasn't occur yet in the non-superconducting diamond, though it is boron-doped, and almost all holes in it are localized at the p-type levels of boron, i.e. it is a dielectric.

of superconducting holes now depends on temperature and decreases monotonically from Δ_0 at $T \ll T_{cr}$ to 0 at $T = T_{cr}$ [29]), the relative permittivity of doped superconducting diamond will be given by the following equation

$$\varepsilon_1 \approx \varepsilon - \frac{\pi N_s \sigma \Delta_0}{\varepsilon_0 N \hbar \omega^2} + i \frac{N_n \sigma}{\varepsilon_0 N \omega}, \quad (2)$$

still referring to $\omega\tau \ll 1$, as it follows from $\omega < 2\Delta/\hbar$, $\Delta \leq \Delta_0$ and $l \ll \xi_0$. The presence of an imaginary part in it (i is the imaginary unit) provides dissipation of plasmon polaritons due to their ohmic absorption by non-superconducting holes. Other numeric values of parameters included in (2) are given in Section 3.

Relative permittivity of the doped diamond, which is close to the insulator–metal phase transition threshold, but is still the insulator, due to the difference between the electric field acting on holes related to acceptors and mean macroscopic field in the Lorentz model [31] is written as

$$\varepsilon_2 = \varepsilon + \frac{N_a \alpha}{1 - N_a \alpha/3}. \quad (3)$$

Here, N_a is the p-type impurity concentration (boron atoms), $\alpha = 4\pi \cdot 4.5 r_B^3$ [32] is the static polarizability of the p-type atom considered as a hydrogen atom in a continuous medium with the relative permittivity ε, $r_B = 4\pi\varepsilon_0\hbar^2\varepsilon/(me^2)$ is its Bohr radius.

2. Surface plasmon polariton dispersion law and eigen frequencies of localized states of plasmon polaritons

The law of dispersion of plasmon polaritons, electromagnetic field of which is proportional to $\exp(-i\omega t + i\mathbf{kr})$, where t is the time, $\mathbf{k}$ is the wave vector, $\mathbf{r}$ is the radius vector, is given by equation [1]:

$$k_{\parallel} = \sqrt{\varepsilon_0 \mu_0}\omega \sqrt{\frac{\varepsilon_1 \varepsilon_2}{\varepsilon_1 + \varepsilon_2}}. \quad (4)$$

Here, μ_0 is the magnetic constant, relative magnetic permeability of the diamond lattice is very close to unity [33] and therefore its variation from unity is neglected, $k_{\parallel}$ is the wave vector projection on the superconducting and non-superconducting doped diamond interface plane.

Wave vector projections on direction orthogonal to this plane (corresponding axis is directed from the non-superconducting to superconducting doped diamond) are written as

$$k_{\perp 1} = -\frac{\sqrt{\varepsilon_0 \mu_0} i\omega\varepsilon_1}{\sqrt{-(\varepsilon_1 + \varepsilon_2)}} \text{ and } k_{\perp 2} = -\frac{\sqrt{\varepsilon_0 \mu_0} i\omega\varepsilon_2}{\sqrt{-(\varepsilon_1 + \varepsilon_2)}} \quad (5)$$

in superconducting and non-superconducting doped diamond, respectively. It can be seen from them that with unlike signs of $\mathrm{Re}\varepsilon_1$ and ε_2 (i.e. $\mathrm{Re}\varepsilon_1 < 0$, $\varepsilon_2 > 0$) and $|\mathrm{Re}\varepsilon_1| \gg |\mathrm{Im}\varepsilon_1|$, imaginary parts of $k_{\perp 1}$ and $k_{\perp 2}$ will also have unlike signs. This allows exponential decay of electromagnetic field and related polarization of the surface plasmon polariton in both sides from the interface plane.

Value $k_{\parallel}$ (4) with $\mathrm{Re}\varepsilon_1 < 0$, $|\mathrm{Re}\varepsilon_1| \gg |\mathrm{Im}\varepsilon_1|$ is almost purely imaginary with $\mathrm{Re}(\varepsilon_1) + \varepsilon_2 > 0$ and purely real with $\mathrm{Re}(\varepsilon_1) + \varepsilon_2 < 0$. Thus, persistent surface plasmon polaritons can basically exist only when the absolute value of the negative real part of permittivity doped diamond (1) and (2) is higher than the positive dielectric permittivity of non-superconducting doped diamond (3). However, they will almost always have a finite propagation length defined, for example, by scattering by lattice defects and interface nonuniformities, including in conventional electromagnetic waves (radiation-induced loss).

Point $\mathrm{Re}\varepsilon_1 + \varepsilon_2 = 0$ itself, referred to as the plasmon polariton resonance, formally corresponds to infinitely small wavelength of the surface plasmon polariton along the interface plane and infinitely small decay scale of plasmon polariton in direction orthogonal to this plane. Actually, the employed equations in this point and some its neighborhood from $\mathrm{Re}\varepsilon_1 + \varepsilon_2 < 0$ become inapplicable because the neglected space dispersion of permittivity, i.e. it was supposed that $kl \leq 1$ (see above). Therefore k calculated using these equations shall satisfy $kl \leq 1$, and direct neighborhood of point $\mathrm{Re}\varepsilon_1 + \varepsilon_2 = 0$ of plasmon polariton resonance from $\mathrm{Re}\varepsilon_1 + \varepsilon_2 < 0$, where this condition is broken, cannot be described using these equations.

When considering localized states of surface plasmon polaritons on the superconducting dope diamond nanoparticles in the non-superconducting doped diamond, these particles are considered to be spherical. Their radius defining the typical scale of change of the electric field and polarization shall exceed $l \approx 1\,\mathrm{nm}$ [28] for validity of neglecting the space dispersion of permittivity. Eigen frequencies of such localized states of surface plasmon polaritons are known to be found from equation $\varepsilon_1 = -2\varepsilon_2$ [1], and are also complex with complex ε_1, reflecting ohmic dissipation of their energy.

In addition, however, for localized states of surface plasmon polaritons, there is another source of decay which is associated with radiation loss and is neglected in this equation derived in quasistatic approximation. Therefore, focus shall also be made on localized states of surface plasmon polaritons on the non-superconducting doped diamond nanoparticles in the superconducting doped diamond. Their eigen frequencies are found from $\varepsilon_1 = -\varepsilon_2/2$ [1], and are also complex with complex ε_1, reflecting ohmic dissipation of their energy. However, due to negativeness of $\mathrm{Re}\varepsilon_1$ (and, consequently, of impossibility of wave propagation in the superconducting doped diamond at these eigen frequencies), such localized states of surface plasmon polaritons have no additional radiation-induced loss of energy. Therefore, their resonance lines will be narrower and, consequently, it is better to use them for high-sensitivity measurements of ε_2 by the shift of these lines. However, it will be harder to accomplish excitation and detection of such localized states of surface plasmon polaritons. Therefore,

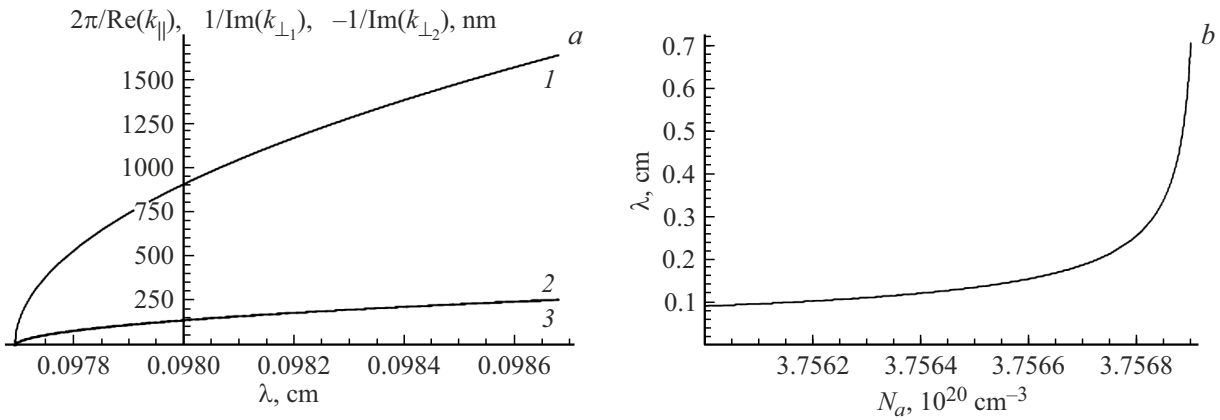

Figure 1. Low temperature $T \ll T_{cr}$ case: *a* — dependence of surface plasmon polariton wavelength $2\pi/k_{\|}$ (curve *1*) and localization scales in the transverse coordinate in the superconducting doped diamond $1/\mathrm{Im}(k_{\perp 1})$ (curve *2*) and in the non-superconducting doped diamond $-1/\mathrm{Im}(k_{\perp 2})$ (curve *3*) on $\lambda = 2\pi c/\omega$ corresponding to their frequency ω . Lower limit λ in the diagram corresponds to $\omega = 2\Delta_0/\hbar$, $N_a = 3.76 \cdot 10^{20}\,\mathrm{cm}^{-3}$, curves *2* and *3* merged together in the adopted scale; *b* — dependence of the vacuum wavelength of localized states of surface plasmon polaritons on non-superconducting doped diamond nanoparticles implanted into the superconducting doped diamond on the boron atom concentration in them N_a.

these nanoparticles shall be probably placed very close to the sample surface.

3. Properties of surface plasmon polaritons and their localized states at the superconducting and non-superconducting doped diamond interface

For heavily boron-doped (to concentration about $10^{21}\,\mathrm{cm}^{-3}$ and higher) diamond, which switches to the superconducting state at temperatures below$T_{cr} \approx 4.2\,\mathrm{K}$ [28], $v \sim 3 \cdot 10^7$ cm/s and, consequently, $\xi_0 \sim 100$ nm are typical. Hence, with $T \ll T_{cr}$, when $N_s \approx N$, $N_n \ll N$, possible frequencies of ohmically dissipativeless surface plasmon polaritons $\omega < 2\Delta_0/\hbar \approx 1.9 \cdot 10^{12}$ rad/s (about 300 GHz), which corresponds to vacuum wavelengths more than 0.97 mm. With properly chosen concentration of acceptors N_a in the non-superconducting doped diamond, $k_{\|}$ (4) and $k_{\perp 1,2}$ (5) can correspond to their wavelengths and localization scale in the transverse coordinate of about 1 nm (i.e. more than one million times smaller than their vacuum wavelengths). These wavelengths and scales are equal to the minimum scale of about $l \sim 1$ nm [28], which, as mentioned above, can be considered within this method, i.e. neglecting space dispersion of permittivity (Figure 1). However, the continuous medium model is still valid because l is much larger than the distance (0.15 nm [30]) between the nearest carbon atoms in the diamond crystal lattice.

Surface plasmon polaritons in the given approximation are ohmically dissipativeless ($\mathrm{Im}k_{\|} = 0$) and, as mentioned above, their propagation length will be determined in practice by scattering by lattice defects and interface nonuniformities. Its estimate depends on the properties of a particular diamond sample and growth technique because it is these factors that define the types and concentrations of these defects and inhomogeneities.

However, note that the superconducting-non-superconducting (and therefore differently doped) diamond interface quality potentially can be much higher than the metal (including superconducting)-dielectric interface, which is generally used for generating surface plasmon polaritons. This is due to the fact that unlike the metal-dielectric interface, the superconducting-non-superconducting doped diamond interface is formed in a continuous epitaxial growth process and modulated diamond-film doping by vapor-phase deposition on single-crystal diamond substrate, and that lattice constants of the superconducting and non-superconducting doped diamonds are very close to each other (according to [34], even if the non-superconducting diamond hadn't been boron-doped, then with a boron atom concentration in the superconducting diamond equal to the value of about $10^{21}\,\mathrm{cm}^{-3}$, which is necessary to achieve superconductivity, the relative difference of lattice constants would have been maximum 0.05 %, i.e. would have been negligibly small). Therefore radiation-induced loss of surface plasmon polaritons caused by their scattering by interface nonuniformities can be much lower for the superconducting-non-superconducting doped diamond than for the normal metal-dielectric interface where they are usually significant and define the surface plasmon polariton propagation length limit [35,36].

Similarly, for localized states of surface plasmon polaritons on the non-superconducting doped diamond nanoparticles implanted into the superconducting doped diamond, decay in the given approximation is equal to zero (their eigen frequency has no imaginary part) and will be actually defined by absorption on lattice imperfections.

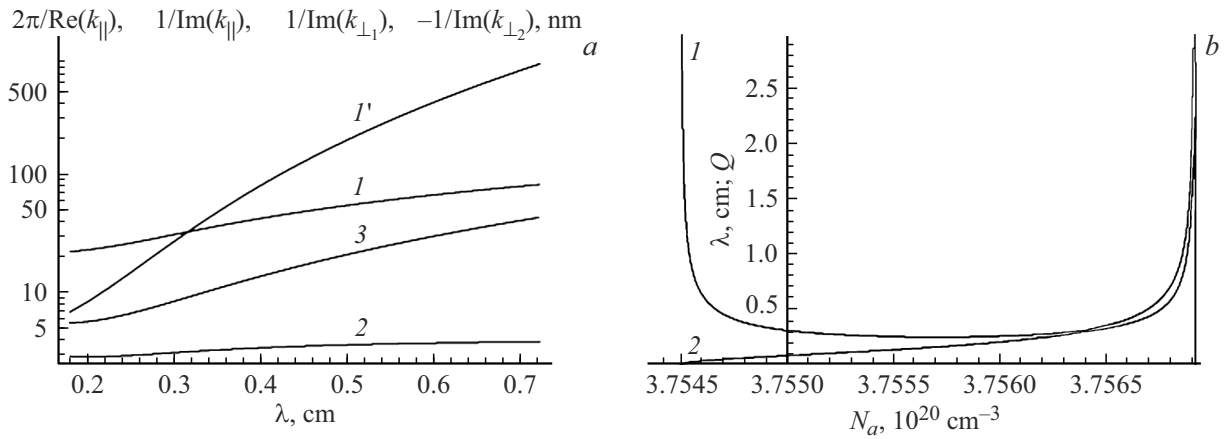

Figure 2. Case of temperatures close to the critical temperature, in particular $T = 0.9T_{cr}$: *a* — dependence of surface plasmon polariton wavelength $2\pi/\mathrm{Re}k_{\|}$ (curve *1*), length of their ohmic decay $1/\mathrm{Im}k_{\|}$ (curve *1′*) and localization scales in the transverse coordinate in the superconducting doped diamond $1/\mathrm{Im}(k_{\perp 1})$ (curve *2*) and in the non-superconducting doped diamond $-1/\mathrm{Im}(k_{\perp 2})$ (curve *3*) on $\lambda = 2\pi c/\omega$ corresponding to their frequency ω. Lower limit λ in the diagram corresponds to $\omega = 2\Delta/\hbar$, $N_a = 3.76 \cdot 10^{20}\,\mathrm{cm}^{-3}$; *b* — dependence of the vacuum wavelength $\lambda = 2\pi c/\mathrm{Re}\omega$ (curve *1*) and Q factor Q (curve *2*) of localized states of surface plasmon polaritons on non-superconducting doped diamond nanoparticles implanted into the superconducting doped diamond on the boron atom concentration in them N_a.

Note also that with $T \ll T_{cr}$ normal dissipative surface plasmon polaritons and their localized states can also exist (as at the interface between the common metal with negative real part of permittivity and dielectric) at higher frequencies, in particular when $\omega\tau \gg 1$ is satisfied. This is due to the fact that when this condition is satisfied, $\omega \gg 2\Delta_0/\hbar$ will be also true, and according to [5], permittivity of the superconducting doped diamond will be equal to the permittivity of a normal (non-superconducting) semiconductor that has changed into a state with metallic type of conductivity.

In other temperature-limiting case, when $T_{cr} - T \ll T_{cr}$, according to the Bardeen–Cooper–Schrieffer theory [29], we have $\Delta \approx 3k_B T_{cr}\sqrt{1 - T/T_{cr}} \ll \Delta_0$, $N_s \approx 2N(1 - -T/T_{cr}) \ll N$, $N_n \approx N$. Surface plasmon polaritons can also exist (Figure 2), but due to a decrease in Δ compared with Δ_0 in condition $\omega < 2\Delta/\hbar$ superimposed on their frequencies, vacuum wavelengths corresponding to the surface plasmon polaritons appear to be higher than in case of $T \ll T_{cr}$. Wavelengths (more than $11\,\mu$m) and localization scales in the transverse coordinate (more than $6\,\mu$m) will be much higher than those for $T \ll T_{cr}$.

Moreover, surface plasmon polaritons are ohmically dissipative even with $\omega < 2\Delta/\hbar$ due to the presence of the imaginary part in ε_1 determined by equation (2). Thus, with $T = 0.9T_{cr}$, their ohmic field absorption length is longer than their wavelength (and, accordingly, they become propagating) only at sufficiently long vacuum wavelengths exceeding 0.32 cm.

Localized states of surface plasmon polaritons on non-superconducting doped diamond nanoparticles implanted into the superconducting doped diamond can also exist with $T_{cr} - T \ll T_{cr}$, but they are also ohmically dissipative (i.e. their eigen frequencies have imaginary parts) due to the presence of the imaginary part in ε_1 (2). Their quality factor $Q = -\mathrm{Re}\omega/(2\pi\mathrm{Im}\omega)$ (minus sign is related to the fact that $\mathrm{Im}\omega < 0$, and Q is defined as a positive value) is higher than 1 only in a narrow range of concentration of the p-type boron atom dopant in non-superconducting diamond nanoparticles (Figure 2, *b*).

At higher frequencies satisfying $\omega\tau \gg 1$ as with $T \ll T_{cr}$, there can be ohmically dissipative surface plasmon polaritons, which are actually no different from normal plasmon polaritons at the interface between the normal metal with negative real part of permittivity and dielectric, or their localized states on dielectric (metal) particles implanted into the metal (dielectric).

Summarizing this section, it should be noted that when equation (6) from [37], which is more exact than equation (3), is used for the permittivity of a doped diamond, which is near the insulator–metal phase transition threshold, but is still an insulator, optimum concentrations of the p-type boron atom impurity N_a in it are 2.5 times lower than the values about $3.76 \cdot 10^{20}\,\mathrm{cm}^{-3}$ obtained in this work. However, due to the approximated description of neutral p-type boron atoms by the hydrogen atom model in continuous dielectric medium with relative permittivity of pure diamond, on which both equations are based, this refinement can go beyond the accuracy of these equations. Therefore, the found optimum N_a shall be treated as order-of-magnitude estimates, and their more accurate values shall be determined from experiment with particular diamond samples grown using a particular technique.

Conclusion

Thus, it is shown that surface plasmon polaritons can exist at the boron-doped non-superconducting and superconducting diamond interface. However, they can have

simultaneously high space localization with a scale up to 1 nm compared with wavelengths in continuous media, which correspond to their frequencies, and low absorption defined by high quality of sample lattice. Also, localized states of surface plasmon polaritons with high Q quality factor can exist on non-superconducting doped diamond nanoparticles implanted into the superconducting doped diamond. Such combination of high localization and low absorption of plasmon polaritons is unique and unattainable for the dielectric-non-superconducting metal interface due to the finite conductivity of the latter. It is also unattainable for the dielectric-superconducting metal interface due to its defect structure induced by misalignment of their lattice parameters. Thus, surface plasmon polaritons well-known for interfaces between dielectrics and normal or superconducting metals may be of much greater interest for applications in case of interface between the boron-doped superconducting and non-superconducting diamonds.

Funding

This study was carried out under the state order of the Federal Research Center - Institute of Applied Physics named after A.V.Gaponov-Grekhov, Russian Academy of Sciences, project FFUF-2024-0032.

Conflict of interest

The authors declare no conflict of interest.

References

[1] S.A. Maier. *Plasmonics: Fundamentals and Applications* (Springer-Verlag, Berlin, 2007)
[2] M.T. Hill, M. Marell, E.S.P. Leong, B. Smalbrugge, Y. Zhu, M. Sun, P.J. van Veldhoven, E.J. Geluk, F. Karouta, Y.S. Oei, R. Notzel, C.-Z. Ning, M.K. Smit. Opt. Express, **17** (13), 11107 (2009). DOI: 10.1364/OE.17.011107
[3] R.F. Oulton, V.J. Sorger, T. Zentgraf, R.M. Ma, C. Gladden, L. Dai, G. Bartal, X. Zhang. Nature, **461**, 629 (2009). DOI: 10.1038/nature08364
[4] M.A. Noginov, G. Zhu, A.M. Belgrave, R. Bakker, V.M. Shalaev, E.E. Narimanov, S. Stout, E. Herz, T. Suteewong, U. Wiesner. Nature, **460** (7259), 1110 (2009). DOI: 10.1038/nature08318
[5] A.A. Abrikosov, L.P. Gor'kov. Sov. Phys. JETP, **35** (6), 1090 (1959).
[6] D.A. Kirzhnits, E.G. Maksimov, D.I. Khomskii. J. Low Temp. Phys., **10** (1/2), 79 (1973). DOI: https://doi.org/10.1007/BF00655243
[7] V.L. Ginzburg, D.A. Kirzhnits (editors). *The Problem of High-Temperature Superconductivity* (Springer, Berlin, 1982)
[8] Q. Buisson, P. Xavier, J. Richard. Phys. Rev. Lett., **73** (23), 3153 (1994). DOI: 10.1103/PhysRevLett.73.3153
[9] A. Das Arulsamy. Appl. Phys. B, **131**, 103 (2025). DOI: 10.1007/s00340-025-08454-7
[10] A. Thomas, E. Devaux, K. Nagarajan, T. Chervy, M. Seidel, G. Rogez, J. Robert, M. Drillon, T.T. Ruan, S. Schlittenhardt, M. Ruben, D. Hagenmüller, S. Schütz, J. Schachenmayer, C. Genet, G. Pupillo, T.W. Ebbesen. J. Chem. Phys., **162** (13), id.134701 (2025). DOI: 10.1063/5.0231202
[11] N. Strugo, K. Balasubramanian, D. Panna, A. Hayat. Opt. Lett., **45** (7), 2062 (2020). DOI: 10.1364/OL.387928
[12] A.S. Abramov, I.O. Zolotovskii, D.I. Sementsov. Opt. Spectr., **119** (5), 875 (2015). DOI: 10.1134/S0030400X15100021
[13] M. Li, Z. Dai, W. Cui, Z. Wang, F. Katmis, J. Wang, P. Le, L. Wu, Y. Zhu. Phys. Rev. B, **89** (23), 235432 (2014). DOI: 10.1103/PhysRevB.89.235432
[14] O.L. Berman, Y.E. Lozovik, A.A. Kolesnikov, M.V. Bogdanova, R.D. Coalson. J. Opt. Society America B, **30** (4), 909 (2013). DOI: 10.1364/JOSAB.30.000909
[15] A. Tsiatmas, A.R. Buckingham, V.A. Fedotov, S. Wang, Y. Chen, P.A.J. de Groot, N.I. Zheludev. Appl. Phys. Lett., **97** (11), 111106 (2010). DOI: 10.1063/1.3489091
[16] M. Imada, A. Fujimori, Y. Tokura. Rev. Mod. Phys., **70** (4), 1039 (1998). DOI: 10.1103/RevModPhys.70.1039
[17] D. Pines. Phys. Rev., **109** (2), 280 (1958). DOI: 10.1103/PhysRev.109.280
[18] M.L. Cohen. Phys. Rev., **134** (2A), A511 (1964). DOI: 10.1103/PhysRev.134.A511
[19] M.L. Cohen. Rev. Mod. Phys., **36** (1), 240 (1964). DOI: 10.1103/RevModPhys.36.240
[20] M.L. Cohen, R.D. Parks (editor). *Superconductivity* (Marcel Decker, NY., 1964), v. 1, p. 615.
[21] R.A. Hein, J.W. Gibson, R. Mazelsky, R.C. Miller, J.K. Hulm. Phys. Rev. Lett., **12** (12), 320 (1964). DOI: 10.1103/PhysRevLett.12.320
[22] R.A. Hein, J.W. Gibson, R.S. Allgaier, B.B. Jr. Houston, R. Mazelsky, R.C. Miller, J.G. Daunt, D.O. Edwards, F.J. Milford, M. Yaquab (editors). *Low Temperature Physics, LT9* (Plenum Press, NY., 1965), p. 604.
[23] J.F. Schooley, W.R. Hosler, M.L. Cohen. Phys. Rev. Lett., **12** (17), 474 (1964). DOI: 10.1103/PhysRevLett.12.474
[24] E.A. Ekimov, V.A. Sidorov, E.D. Bauer, N.N. Mel'nik, N.J. Curro, J.D. Thompson, S.M. Stishov. Nature, **428**, 542 (2004). DOI: 10.1038/nature02449
[25] J. Scharpf, A. Denisenko, C.I. Pakes, S. Rubanov, A. Bergmaier, G. Dollinger, C. Pietzka, E. Kohn. Phys. Status Solidi A, **210** (10), 2028 (2013). DOI: 10.1002/pssa.201300093
[26] H. El-Hajj, A. Denisenko, A. Bergmaier, G. Dollinger, M. Kubovic, E. Kohn. Diamond Relat. Mater., **17** (4–5), 409 (2008). DOI: 10.1016/j.diamond.2007.12.030
[27] V.V. Schmidt. *The Physics of Superconductors: Introduction to Fundamentals and Applications* (Springer-Verlag, Berlin, 1997)
[28] E. Bustarret, S. Koizumi, C. Nebel, M. Nesladek (editors). *Physics and Applications of CVD Diamond* (WILEY-VCH Verlag GmbH & Co. KGaA, Weinheim, 2008), p. 329.
[29] E.M. Lifshitz, L.P. Pitaevsky. *Theoretical Physics. Vol. IX. Statistical Physics. Part 2. Condensed Matter Theory* (Butterworth-Heinemann, Oxford, 2002)
[30] O. Madelung. *Semiconductors: Data Handbook* (Springer, Berlin, 2004)
[31] N.F. Mott. *Metal–Insulator Transitions* (Taylor & Francis, London-NY., 1990)

[32] L.D. Landau, E.M. Lifshitz. *Theoretical Physics. Vol. III. Quantum Mechanics: Non-relativistic Theory* (Butterworth-Heinemann, Oxford, 2003)
[33] N.V. Novikov (red.). *Fizicheskie svoistva almaza*. Spravochnik (Naukova dumka, Kiev, 1987) (in Russian)
[34] V.V. Brazhkin, E.A. Ekimov, A.G. Lyapin, S.V. Popova, A.V. Rakhmanina, S.M. Stishov, V.M. Lebedev, Y. Katayama, K. Kato. Phys. Rev. B, **74** (14), 140502(R) (2006). DOI: 10.1103/PhysRevB.74.140502
[35] V.V. Gerasimov, B.A. Knyazev, A.G. Lemzyakov, A.K. Nikitin, G.N. Zhizhin. J. Opt. Soc. Am. B, **33** (11), 2196 (2016). DOI: 10.1364/JOSAB.33.002196
[36] V.V. Gerasimov A.K. Nikitin, V.S. Vanda, A.G. Lemzyakov, I.A. Azarov. J. Infrared Milli Terahz Waves, **46**, 32 (2025). DOI: 10.1007/s10762-025-01051-x
[37] N.A. Poklonski, S.A. Vyrko, A.G. Zabrodskii. Solid State Physics, **46** (6), 1101 (2004). DOI: 10.1134/1.1767252

Translated by E.Ilyinskaya